Diffraction at HERA

Alexander Proskuryakov

Moscow State University, 119889 Moscow, Russia

Abstract

Recent results from HERA on diffraction are reviewed. Exclusive electroproduction of vector mesons is presented and compared to the QCD based models. The measurement of the diffractive structure function is discussed. The dijet production is analysed and compared to the resolved Pomeron model.

1 Introduction

This paper reports the recent results on diffraction at HERA from the H1 and ZEUS collaborations. A detailed description of experimental data on diffractive scattering in hadron-hadron interactions is available in [1].

Diffractive dissociation of the real photon in the reaction $\gamma p \to Xp$ was studied in fixed target experiments up to $\sqrt{s} = 14$ GeV [2]. At HERA the study of photon diffractive dissociation in the electroproduction reaction $ep \to eXp$ at very small Q^2 has been extended up to photon-proton centre of mass energy $W =$ 231 GeV [3]. It was found that at low photon virtualities the reaction $\gamma^\star p \to Xp$ has the characteristics of a soft diffractive process: the differential cross section $d\sigma/dtdM_X^2$ at low mass M_X is dominated by the production of vector mesons; above the resonance region the cross section is roughly described by a $1/M_X^2$ dependence; the t distribution is well reproduced by a form e^{bt} for $t < 0.3$ GeV^2; the total diffractive cross section is a slow function of energy. The main properties of these diffractive reactions have found a natural explanation in the framework of the Regge phenomenology [4]. In this approach the reaction is described at high energies via the exchange of a Pomeron trajectory parameterized as $\alpha(t) = \alpha(0) + \alpha' t = 1.08 + 0.25t$ [5].

With the high energy electron-proton collider HERA, it has become possible to study diffractive dissociation initiated by a virtual photon in a wide range of Q^2, and the photon-proton centre-of-mass energy. One of the major results which came from HERA was the observation of the deep inelastic scattering (DIS) events with a large rapidity gap in the hadronic final state. The fraction of such events is practically independent of W and Q^2, and of the order of 10%.

The presence of diffractive events at large Q^2 opens the possibility of describing such events in the framework of QCD. In the approach developed in [7], the diffractive cross section factorizes into the Pomeron flux and the virtual photon-pomeron interaction. The Pomeron is assumed to consist of partons in the same way as the usual hadrons. This leads to a concept of the diffractive parton distributions. In another class of the QCD based models (for a review see [6]) the diffractive process is often viewed in the rest frame of the proton. A hadronic fluctuation of the virtual photon scatters off the proton without color exchange, leading to a rapidity gap in the hadronic final state.

Exclusive vector meson production, being a simple sub-process of the inclusive reaction $ep \to eXp$, offers an unique opportunity to study diffraction. The reaction $ep \to eVp$, where V stands for a vector meson (ρ^0, ω, ϕ, J/ψ, Υ), has been studied at HERA in a wide range of Q^2, W and t. A detailed review of vector meson production at HERA can be found in [8].

This paper is organized as follows. In Section 2 the basic kinematic variables and the diffractive event selection are discussed. Section 3 describes the results on exclusive vector meson production. The measurement of the diffractive structure function and the properties of the hadronic final states are discussed in Section 4.

A more detailed review of the HERA results can be found in [9].

2 Kinematics and event selection

The Hadron Elektron Ring Anlage (HERA) is an electron proton collider operated at a proton energy of 820 GeV and an electron (positron) energy of 27.5 GeV, giving a total centre of mass energy $\sqrt{s} \simeq 300$ GeV.

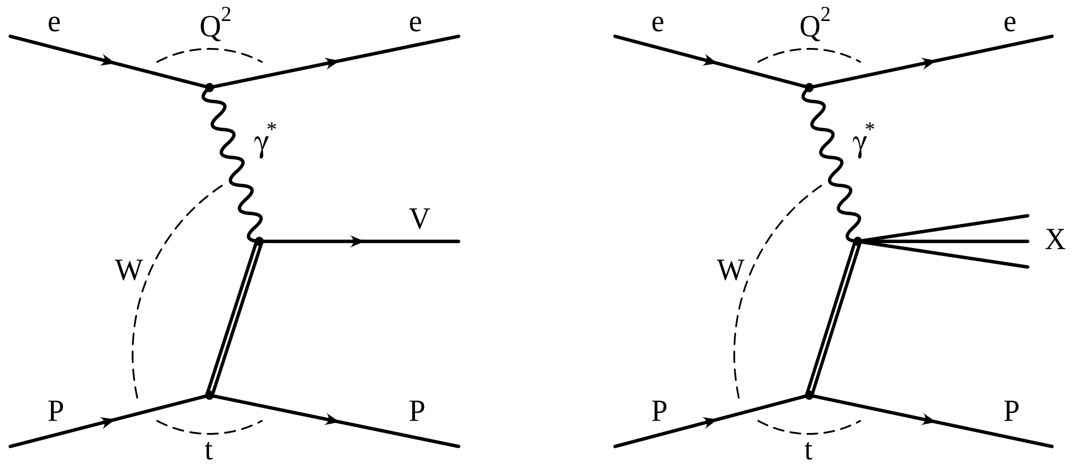

Figure 1: Schematic diagram for exclusive vector meson production and inclusive diffractive scattering in ep interactions.

Figure 1 shows a schematic diagrams for exclusive vector meson production and inclusive diffractive scattering in ep interactions. The kinematics of the reaction $ep \to eVp$, where V stands for a vector meson (ρ^0, ω, ϕ, J/ψ, Υ), is described by the following variables:

- the negative of the four-momentum squared of the exchanged photon, $Q^2 = -(k-k')^2$, where $k(k')$ is the four-momentum of the incident (scattered) electron;
- the centre-of-mass energy of the photon-proton system, $W = \sqrt{(q+P)^2}$, where q and P are the four-momenta of the exchanged photon and the incident proton respectively; the Bjorken variable $y = pq/pk$;
- the four-momentum transfer squared at the proton vertex, $t = (P-P')^2$, where P' is the four-momentum of the scattered proton;
- the angle between the vector meson production plane and the electron scattering plane, Φ.

The kinematics of the vector meson decay (in the following only two particle decay is considered) is described by the polar angle θ and the azimuthal angle ϕ in the s-channel helicity frame [10], in which the quantisation axis is defined as the direction of the momentum of the final-state proton in the V rest frame.

In addition to the previously introduced variables, Q^2, W and t, two more quantities are used to describe the diffractive reaction $ep \to eXp$:

- $x_{I\!P} = \frac{(P-P')q}{Pq} \simeq \frac{M_X^2+Q^2}{W^2+Q^2}$,
- $\beta = \frac{Q^2}{2(P-P')q} \simeq \frac{Q^2}{M_X^2+Q^2}$,

where M_X is the invariant mass of the system X.

The selection of diffractive events in neutral current, deep-inelastic scattering is based on the mesuarement of the scattered electron in the final state. The reaction of exclusive vector meson production is identified by the presence of exactly two oppositely-charged tracks in the tracking detector.

For the selection of the inclusive diffractive reaction $ep \to eXp'$ three different methods have been used at HERA:

- a large rapidity gap was required between the hadronic final state systems X and p', where p' can be the low mass proton dissociative system not detected directly;
- the diffractive contribution was identified as the excess of events at small M_X in the lnM_X^2 distribution [11];
- the diffractive events were selected by detection of a proton in the leading proton spectrometer with a large fraction of the momentum of the incoming proton [12].

3 Vector meson production

3.1 The W dependence of the $\gamma^\star p \to Vp$ cross sections

The differential electron-proton cross section is related to the virtual photon-proton cross section as:

$$\frac{d\sigma^{ep}}{dydQ^2} = \Gamma_T(y, Q^2)\sigma(\gamma^\star p \to Vp), \tag{1}$$

where $\Gamma_T(y, Q^2)$ if the flux of virtual photons [13]. The virtual photon-proton cross section, $\sigma(\gamma^\star p \to Vp) = \sigma_T^{\gamma^\star p} + \epsilon\sigma_L^{\gamma^\star p}$, has contributions from longitudinal (helicity 0 state) and transverse (helicity ± 1 state) photons. In the kinematic region covered by the HERA data the value of the polarization parameter ϵ is close to unity.

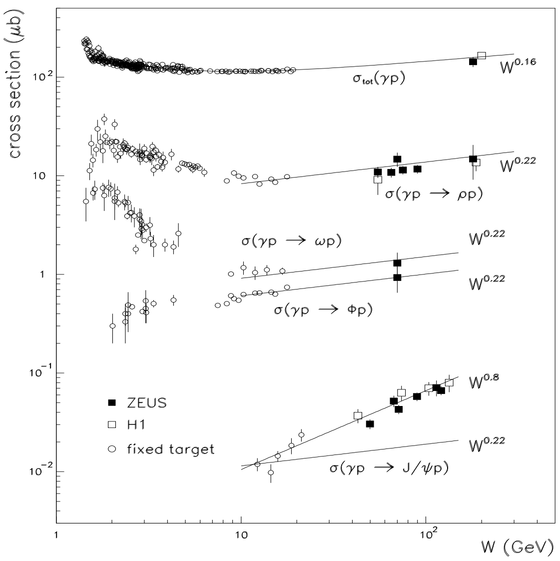

Figure 2: The energy dependence of the vector meson photoproduction cross sections for fixed target and HERA experiments.

Figure 2 shows the energy dependence of elastic ρ^0, ω, ϕ and J/ψ photoproduction ($Q^2 \simeq 0$ GeV^2) cross sections measured at HERA and fixed target experiments. The W dependence of the cross section for light vector meson photoproduction is well parameterized at high energy as $\sigma^{\gamma p} \propto W^\delta$ with $\delta \simeq 0.22$. This weak energy dependence is in agreement with the 'soft' Pomeron exchange prediction $d\sigma/dt \propto (W^2)^{2(\alpha_{I\!P}(t)-1)}$.

In contrast, the energy of the elastic J/ψ photoproduction cross section, shown in Fig. 3, exhibits a steep rise with W. The W dependence of $\gamma p \to J/\psi p$ cross section is described by the function $\sigma^{\gamma p} \propto W^\delta$ with

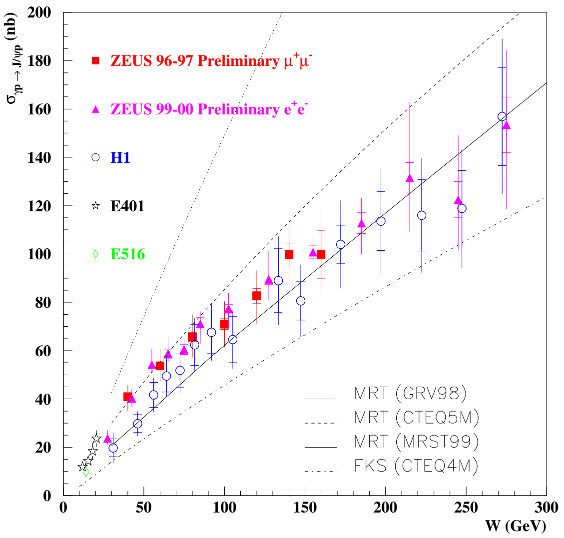

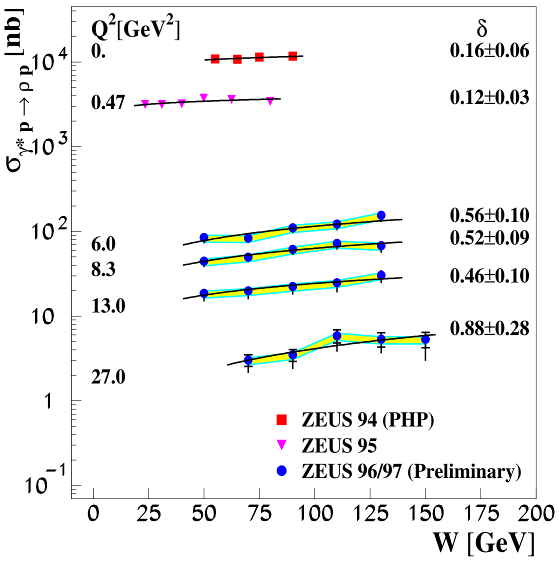

Figure 3: The energy dependence of the elastic J/ψ photoproduction cross section for fixed target and HERA experiments.

Figure 4: The energy dependence of exclusive ρ^0 production cross sections for different values of Q^2. The lines represent the function $\sigma \propto W^\delta$ fitted to the data.

$\delta \simeq 0.8 - 0.9$. This energy dependence is consistent with a perturbative QCD calculation [14], where the hard scale is given by the charm quark mass.

The hard scale can also be provided by the photon virtuality Q^2. Exclusive electroproduction at high values of Q^2 has been the subject of many theoretical investigations (see e.g. [15]). The main prediction of the perturbative QCD models is a fast increase of the cross section with W, connected with the Q^2 evolution of the gluon density of the proton $xg(x, Q^2)$.

The W dependence of the exclusive ρ^0 production cross section at different values of Q^2 is shown in Fig. 4. The lines represent the result of a fit to the data with a function of type $\sigma \propto W^\delta$. As can be seen from Fig. 4, the W dependence of the cross section for the reaction $\gamma^\star p \to Vp$ is consistent with the 'soft' Pomeron approach at low values of Q^2. In the region of high Q^2, where QCD based models predict a steeper cross section dependence on W, the rise of the cross section becomes faster.

3.2 The t dependence of the $\gamma^\star p \to Vp$ cross sections

The exponential t dependence of the $\gamma^\star p \to Vp$ cross section is a typical characteristic of diffractive processes. The slope parameter b, which is related in optical models to the sizes of the interacting particles, is expected to depend on the photon virtuality. Figure 5 shows the slope parameter for exclusive ρ production as a function of Q^2. Despite large statistical errors of the experimental data these results indicate that the slope b decreases with Q^2, approaching the value of $b \simeq 4 - 5$ GeV^{-2}.

The slope parameter also depends on the vector meson mass. The value of b is [16, 17] $9.8 \pm 0.8(\text{stat}) \pm 1.1(\text{syst})$ GeV^{-2}, $7.3 \pm 1.0(\text{stat}) \pm 0.8(\text{syst})$ GeV^{-2} and $4.0 \pm 0.4(\text{stat})^{+0.6}_{-0.7}(\text{syst})$ GeV^{-2}, for photoproduction of ρ^0, ϕ and J/ψ mesons respectively.

3.3 Decay angular distributions

The analysis of vector meson decay distribution provides important information about helicity properties of the reaction $\gamma^\star p \to Vp$. In the case of unpolarized beams, the angular distributions can be written

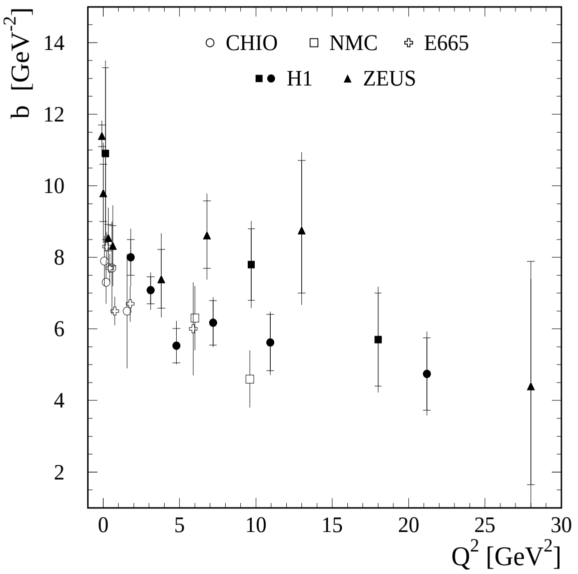

Figure 5: The slope parameter b as a function of Q^2 for exclusive ρ^0 production.

as [10]:

$$
\begin{aligned}
W(\cos\theta,\phi,\Phi) = \tfrac{3}{4\pi}\Big[& \tfrac{1}{2}(1-r^{04}_{00}) + \tfrac{1}{2}(3r^{04}_{00}-1)\cos^2\theta \\
& -\sqrt{2}\mathrm{Re}\{r^{04}_{10}\}\sin 2\theta\cos\phi - r^{04}_{1-1}\sin^2\theta\cos 2\phi \\
& -\epsilon\cos 2\Phi(r^1_{11}\sin^2\theta + r^1_{00}\cos^2\theta - \sqrt{2}\mathrm{Re}\{r^1_{10}\}\sin 2\theta\cos\phi - r^1_{1-1}\sin^2\theta\cos 2\phi) \\
& -\epsilon\sin 2\Phi(\sqrt{2}\mathrm{Im}\{r^2_{10}\}\sin 2\theta\sin\phi + \mathrm{Im}\{r^2_{1-1}\}\sin^2\theta\sin 2\phi) \\
& +\sqrt{2\epsilon(1+\epsilon)}\cos\Phi(r^5_{11}\sin^2\theta + r^5_{00}\cos^2\theta \\
& -\sqrt{2}\mathrm{Re}\{r^5_{10}\}\sin 2\theta\cos\phi - r^5_{1-1}\sin^2\theta\cos 2\phi) \\
& +\sqrt{2\epsilon(1+\epsilon)}\sin\Phi(\sqrt{2}\mathrm{Im}\{r^6_{10}\}\sin 2\theta\sin\phi + \mathrm{Im}\{r^6_{1-1}\}\sin^2\theta\sin 2\phi)\Big].
\end{aligned} \tag{2}
$$

The spin-density matrix elements r^{04}_{ij}, r^{α}_{ij} are the combinations of the helicity amplitudes $T_{\lambda_V,\lambda_\gamma}$, where λ_V and λ_γ are the helicities of the vector meson and the photon respectively. The low energy data indicate that the amplitude for the photon- vector meson transition is dominantly s-channel helicity conserving, i.e. the helicity of the vector meson is equal to that of the photon in the helicity frame. Under the assumption of s-channel helicity conservation (SCHC) the ratio $R = \sigma_L^{\gamma^\star p}/\sigma_T^{\gamma^\star p}$ can be determined via

$$R = \frac{1}{\epsilon}\frac{r^{04}_{00}}{1-r^{04}_{00}}. \tag{3}$$

The full set of spin density matrix elements has been measured for exclusive ρ^0 production. The most significant deviation from the expectation of SCHC is observed for the matrix element r^5_{00}. This matrix element is proportional to the interference between the helicity non-flip amplitude T_{00} and the helicity single-flip amplitude T_{01}. The size of this effect can be quantified by the ratio of the helicity single-flip amplitude to the helicity conserving amplitudes $|T_{01}|/\sqrt{|T_{00}|^2+|T_{11}|^2}$, which gives $(8\pm3)\%$ [18]. The result for r^5_{00} is consistent with the prediction of ref. [19].

Figure 6 shows the 15 spin density matrix elements as a function of Q^2. The results of the QCD based calculations [20, 21] shown in Fig. 6 are in good agreement with the data.

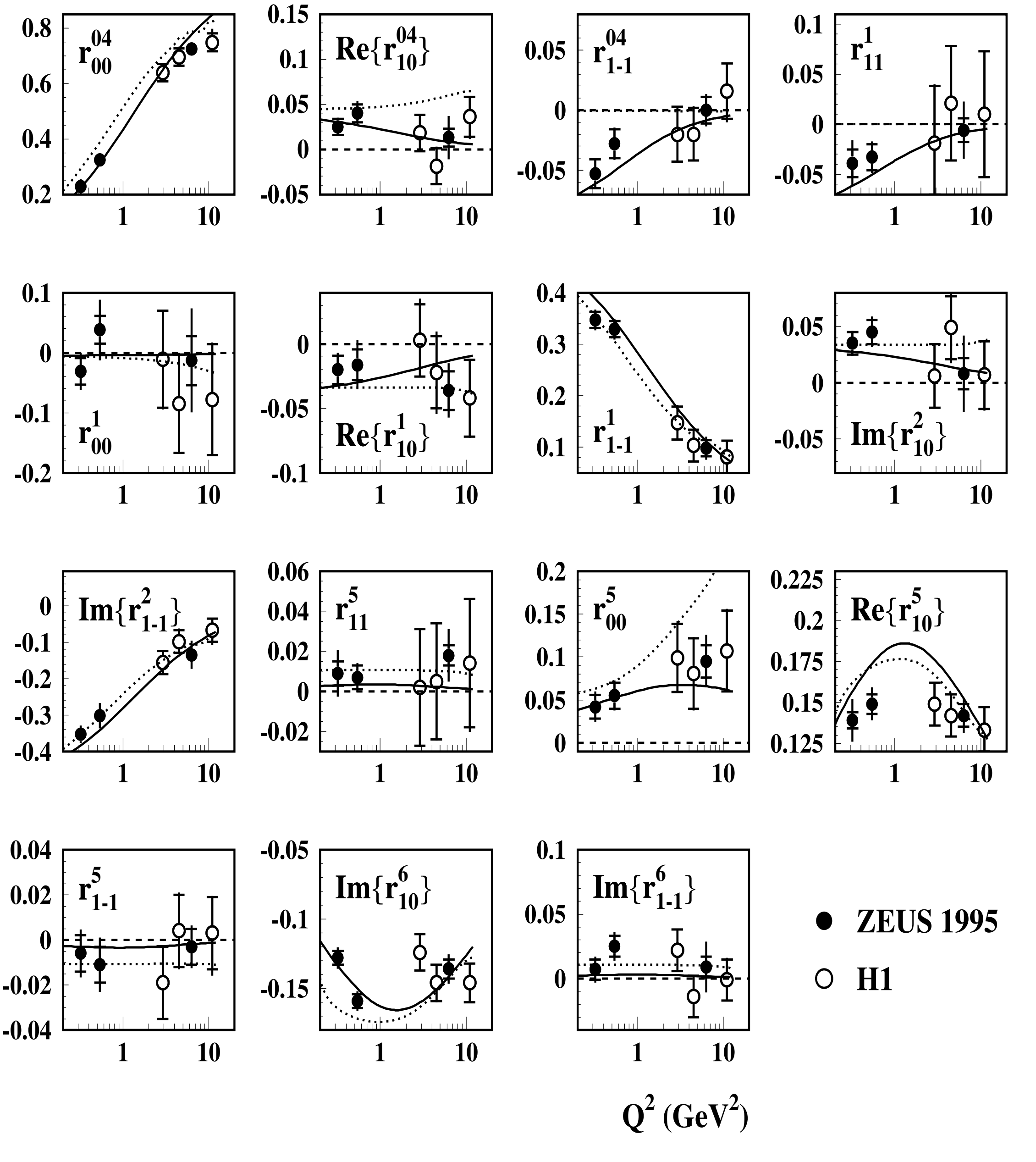

Figure 6: The 15 spin density matrix elements as a function of Q^2. The full curves are the prediction of Ref. [20], the dotted curves the prediction of Ref. [21]. The dashed lines indicate the expectation of SCHC.

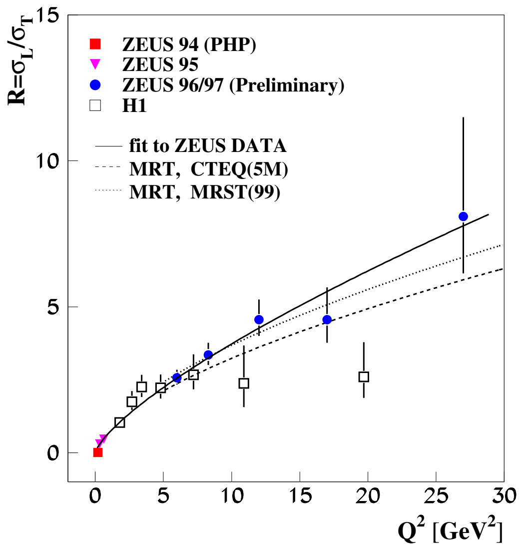

Figure 7: The ratio of the longitudinal and transverse photon-proton cross sections as a function of Q^2. The curves represent the predictions of the QCD [22] based model.

The ratio $R = \sigma_L^{\gamma^* p}/\sigma_T^{\gamma^* p}$, calculated according to eq.(3) (neglecting small violation of SCHC) , is displayed in Fig. 7 as a function of Q^2 for exclusive ρ^0 production. The curves represent the predictions of the QCD [22] based model. Fig.7 shows that the longitudinal photon-proton cross section dominates at large Q^2 and that the non-linear rise of R can be well reproduced by the theoretical models.

4 Inclusive diffraction

4.1 Cross section t dependence

The t distribution in the diffractive reaction $ep \to eXp$ at an average $Q^2 = 8$ GeV^2 has been measured with the leading proton spectrometer [23], which allows the direct determination of the momentum of the scattered proton. It was found that the distribution is well described by a single exponential function with a value of the slope parameter b,

$$b = 7.2 \pm 1.1^{+0.7}_{-0.9} \text{ GeV}^{-2}.$$

For comparison, the slope parameter b, measured in the photoproduction region in the kinematic interval $4 < M_X < 32$ GeV and $176 < W < 225$ GeV was found to be $b = 6.8 \pm 0.9^{+1.2}_{-1.1}$ GeV^{-2} [24].

4.2 Diffractive structure functions and cross section W dependence

In analogy to the DIS cross section, the diffractive $ep \to eXp$ cross section can be written as:

$$\frac{d\sigma^D_{ep}}{d\beta dQ^2 dx_{I\!P} dt} = \frac{2\pi\alpha^2}{\beta Q^4}[1 + (1-y)^2] F_2^{D(4)}(\beta, Q^2, x_{I\!P}, t), \tag{4}$$

where the contribution from the longitudinal structure function is neglected. Usually the cross section is integrated over t and the diffractive processes are analysed in terms of diffractive structure function $F_2^{D(3)}(\beta, Q^2, x_{I\!P}) = \int F_2^{D(4)}(\beta, Q^2, x_{I\!P}, t)dt$.

In the framework of Regge phenomenology the diffractive structure function factorizes into the flux $f_{I\!P}$ of the Pomerons and the structure function $F_2^{I\!P}$:

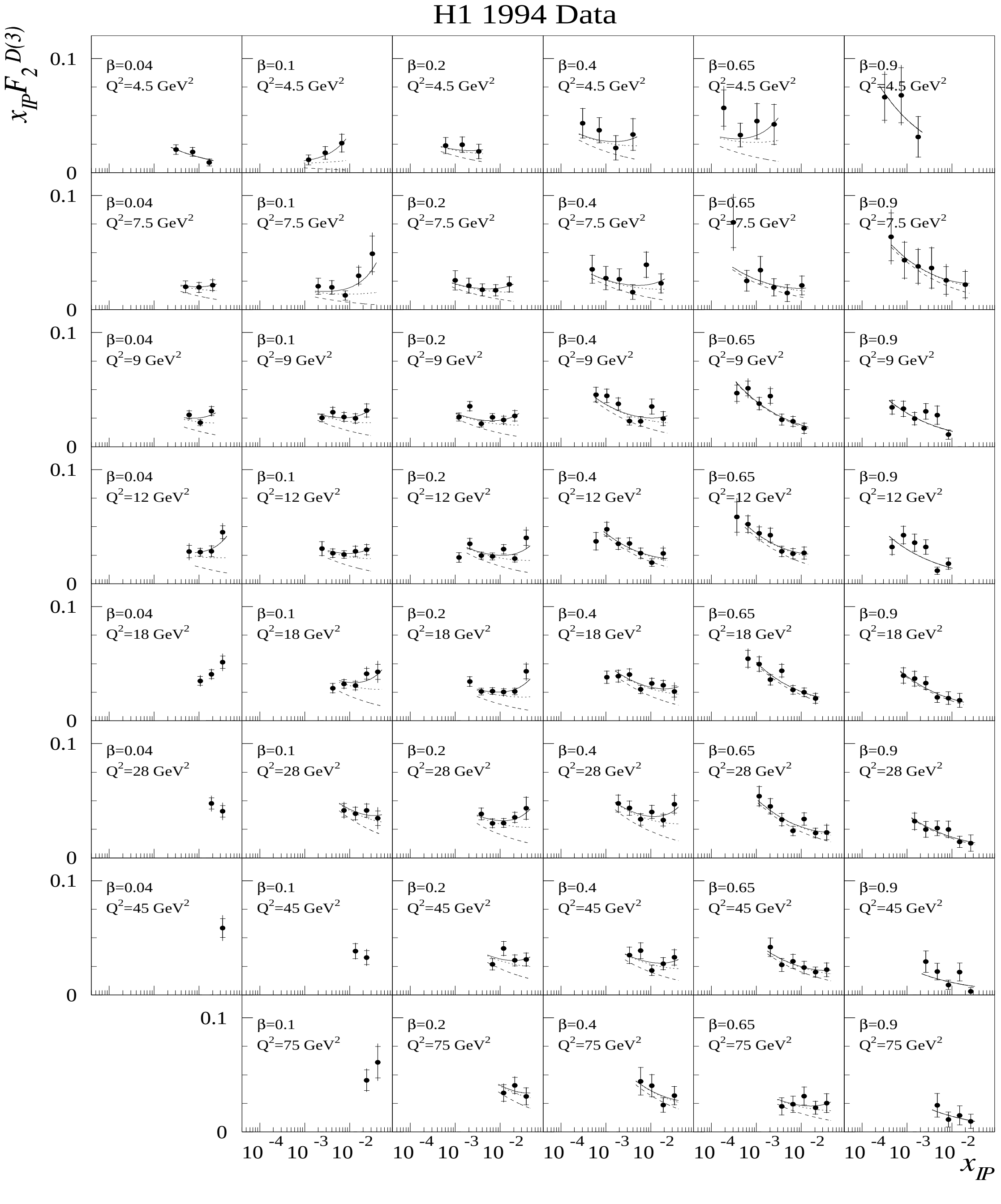

Figure 8: The diffractive structure function $F_2^{D(3)}(\beta, Q^2, x_{I\!P})$ multiplied by $x_{I\!P}$ as a function of $x_{I\!P}$ for various β and Q^2 values.

$$F_2^{D(4)}(\beta, Q^2, x_{I\!P}, t) = f_{I\!P}(x_{I\!P}, t) F_2^{I\!P}(\beta, Q^2), \tag{5}$$

where the flux factor is defined as [7] $f_{I\!P}(x_{I\!P}, t) \sim (1/x_{I\!P})^{2\alpha_{I\!P}(t)-1}$

Figure 8 shows the values of $x_{I\!P} F_2^{D(3)}(\beta, Q^2, x_{I\!P})$ as a function of $x_{I\!P}$ for different values of β and Q^2 [25]. It was found that the exchange of the factorisable Pomeron trajectory, which predicts a universal dependence on $x_{I\!P}$, does not describe the data. However a good description can be achieved assuming the presence of a sub-leading reggeon trajectory in addition to the Pomeron exchange

$$F_2^{D(4)}(\beta, Q^2, x_{I\!P}, t) = f_{I\!P}(x_{I\!P}, t) F_2^{I\!P}(\beta, Q^2) + f_R(x_{I\!P}, t) F_2^R(\beta, Q^2). \tag{6}$$

The value of the Pomeron intercept, extracted from the fit, is

$$\alpha_{I\!P}(0) = 1.203 \pm 0.020(stat) \pm 0.013(syst)^{+0.030}_{-0.035}(model)$$

The intercept of the Pomeron trajectory can also be obtained from the W dependence of the $\gamma^\star p \to Xp$ cross section. Taking into account the fact that $\sigma(\gamma^\star p \to Xp) \sim Q^2 F_2^D$ and that $x_{I\!P} \sim (W^2/M_X^2)$, one can expect a power energy dependence, $\sigma(\gamma^\star p \to Xp) \sim W^a$.

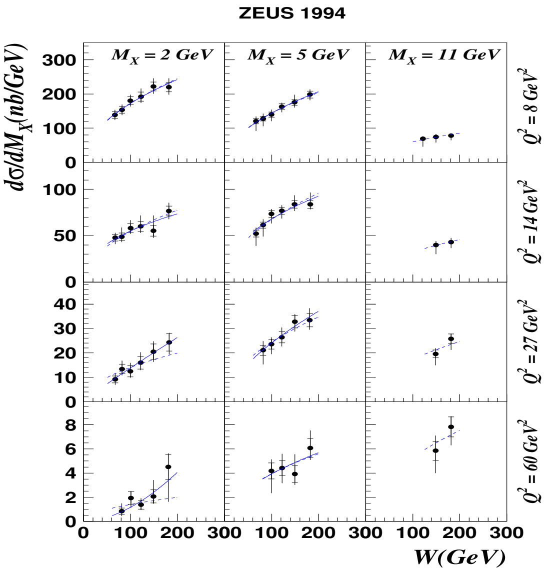

Figure 9: The differential cross section $d\sigma^{diff}_{\gamma^\star p}/dM_X$ as a function of W at different M_X and Q^2 values.

The diffractive cross section as a function of W at different values of M_X and Q^2 is shown in Fig. 9. The cross section was fitted using the form $d\sigma^{diff}_{\gamma^\star p}(M_X, W, Q^2)/dM_X \propto W^a$. The parameter a can be related to the intercept of the Pomeron trajectory through the expression $a = 4(\alpha_{I\!P}(0) - 1 - 0.03)$, where the last term is a correction due to averaging over t. The Pomeron intercept, derived from the fit to the W dependence is $\alpha_{I\!P}(0) = 1.16 \pm 0.01^{+0.04}_{-0.01}$.

The Pomeron intercept extracted from diffractive measurements is shown in Figure 10 as a function of Q^2. The curve is a parameterization of $\alpha_{I\!P}(0)$ derived from the total $\gamma^\star p$ cross section [26]. The diffractive data show less significant dependence on Q^2. In the region of large Q^2 the value of $\alpha_{I\!P}(0)$ is higher than that in the soft interactions.

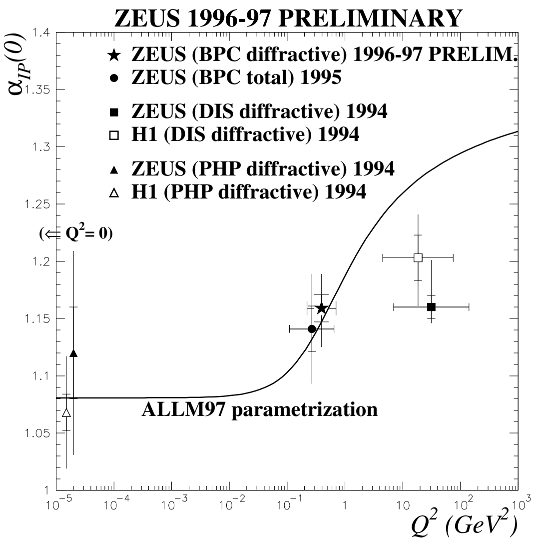

Figure 10: Q^2 dependence of $\alpha_{I\!P}(0)$ extracted from measurements of diffractive and total $\gamma^{\star}p$ cross sections. The curve is a parameterization derived from the total $\gamma^{\star}p$ cross section [26].

4.3 Diffractive parton distributions

The concept of the diffractive parton distributions is based on the QCD factorization theorem which has been proven for the diffractive processes in [27]. This implies that the usual DGLAP equations are valid for the diffractive structure function F_2^D.

A QCD fit was performed to the $F_2^{D(3)}$ measurements [25], using the DGLAP evolution equations. The parton distributions were parameterized at a starting scale of $Q_0^2 = 3$ GeV^2. It was found that the data can not be described if only quarks are assumed to contribute to the structure function at the starting scale. A better description can be achieved by introducing various forms of the gluon distribution at the starting scale. Two solutions (shown in Fig. 11) were found to describe the data. In both fits the fraction of the Pomeron momentum carried by gluons is $\sim 90\%$ at $Q^2 = 4.5$ GeV^2 and $\sim 80\%$ at $Q^2 = 75$ GeV^2.

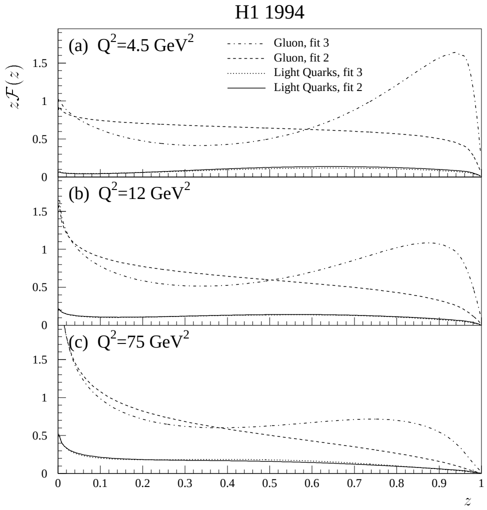

Figure 11: The sum of the light quarks distributions and the gluon distribution for two possible solutions.

4.4 Hadronic final state in diffractive DIS

The study of the hadronic final states in diffractive processes provides an additional information on the partonic structure of diffraction. The production of high p_T jets in diffractive scattering is directly sensitive to the gluon component of t-channel exchange [28]. As an example, the differential cross section

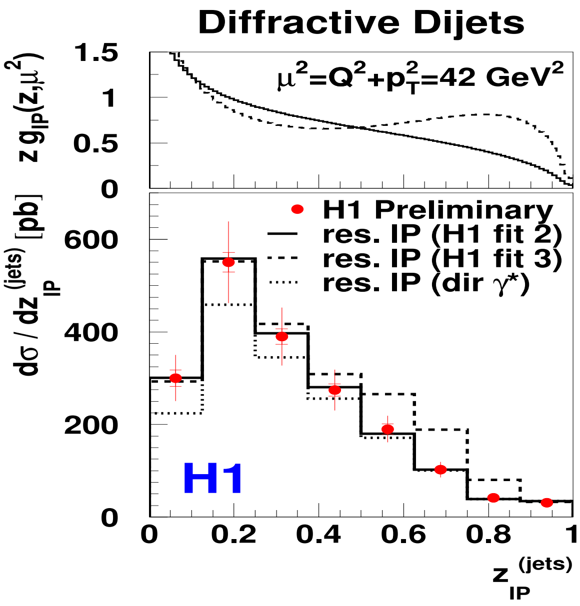

Figure 12:

of dijet production [29] is shown in Fig. 12 as a function of $z_{I\!P} = (M_{JJ}^2 + Q^2)/(M_X^2 + Q^2)$, where M_{JJ} is the mass of the dijet system. The predictions based on the two gluon distributions obtained from the QCD analysis of the diffractive structure function [25] are also presented in the figure. The shape of the differential dijet cross section is sensitive to the shape of the gluon distribution. This constrains the uncertainty of the inclusive measurements and supports the fact that the Pomeron structure is dominated by gluons.

5 Conclusions

The study of diffractive processes at HERA has revived the interest in diffraction. The variety of experimental data available at HERA has opened the opportunity to explore the diffractive scattering in the regions of "soft" and "hard" physics, and to study the transition between these two regimes.

Future running at HERA is expected to significantly improve the precision of the measurements. This, together with the theory development, will deepen our understanding of diffractive phenomena.

Acknowledgements

I would like to thank the organizers of the workshop for its stimulating and enjoyable atmosphere.

References

[1] K. Goulianes, Nucl. Phys. (Pros. Suppl.) B12 (1990) 110.

[2] T.J. Chapin et. al. Phys. Rev. B31 (1985) 17.

[3] H1 Collab., C. Adloff et al., Z. Phys. C74 (1997) 221.

[4] see e.g. P.D.B. Collins, Introduction the Regge Theory and High Energy Physics, Cambridge University Press (1977).

[5] A. Donnachie and P.V. Landshoff, Phys. Lett. B296 (1992) 227.

[6] A. Hebecher, hep-ph/9909504.

[7] G. Ingelman and P.E. Schlein, Phys. Lett. B152 (1985) 256.

[8] J.A. Crittenden, Exclusive Production of Neutral Vector Mesons at the Electron-Proton Collider HERA, Springer Tract in Modern Physics, Volume 140, Springer, Berlin, Heidelberg (1997).

[9] H. Abramowicz and A. Caldwell, Rev. Mod. Phys. 71 (1999) 1275.

[10] K. Schilling, G. Wolf, Nucl. Phys. B61 (1973) 381.

[11] ZEUS Collab., J. Breitweg et al., E. Phys. J. C6 (1999) 43.

[12] ZEUS Collab., J. Breitweg et al., E. Phys. J. C1 (1998) 81.

[13] L.N. Hand, Phys. Rev. 129 (1963) 1834.

[14] M.G. Ryskin, Z. Phys. C57 (1993) 89;
M.G. Ryskin et al., Z. Phys. C76 (1997) 231.

[15] S. Brodsky et al., Phys. Rev. D50 (1994) 3134;
J. Nemchik, N.N. Nikolaev and B.G. Zakharov, Phys. Lett. B341 (1994) 228;
A. Donnachie and P.V. Landshoff, Phys. Lett. B348 (1995) 213;
L. Frankfurt, W. Koepf and M. Strikman, Phys. Rev. D54 (1996) 3194;
A.D. Martin, M.G. Ryskin and T. Teubner, Phys. Rev. D55 (1997) 4329.

[16] ZEUS Collab., M Derrick et al., Z. Phys. C69 (1995) 39;
H1 Collab., S. Aid et al., Nucl. Phys. B463 (1996) 3;
ZEUS Collab., M. Derrick et al., Phys. Lett. B377 (1996) 259;
ZEUS Collab., M. Derrick et al., Z. Phys., C73 (1996) 73;
ZEUS Collab., M. Derrick et al., Z. Phys. C73 (1997) 253;
ZEUS Collab., J. Breitweg et al., Eur. Phys. J. C2 (1998) 247;
ZEUS Collab., J. Breitweg et al., Eur. Phys. J. C6 (1999) 603.

[17] ZEUS Collab., M. Derrick et al., Phys. Lett. B350 (1995) 120;
H1 Collab., S. Aid et al., Nucl. Phys., B472 (1996) 3;
ZEUS Collab., J. Breitweg et al., Z. Phys. C75 (1997) 215.

[18] H1 Collab., C. Adloff et al., DESY 99-010;
ZEUS Collab., J. Breitweg et al., Eur. Phys. J., C12 (2000) 393.

[19] D.Yu. Ivanov and R. Kirschner, Phys. Rev. D58 (1998) 114025.

[20] E.V. Kuraev, N.N. Nikolaev and B.G. Zakharov, JETP Lett. 68 (1998) 696 and Pisma Zh. Eksp. Teor. Fiz. 68 (1998) 667;
N.N. Nikolaev, Proceedings of the DIS99 workshop, April 19-23, 1999, Zeuthen, Germany, Eds. J. Blumlein and T. Riemann, to apper in Nucl. Phys. B (Proc. Suppl.).

[21] I. Royen, Proceedings of the DIS99 workshop, April 19-23, 1999, Zeuthen, Germany, Eds. J. Blumlein and T. Riemann, to apper in Nucl. Phys. B (Proc. Suppl.) and Liege University preprint ULC-PNT-99-1-IR.

[22] A.D. Martin, M.G. Ryskin and T. Teubner, hep-ph/9912551.

[23] ZEUS Collab., paper submitted to the European Conference on High Energy Physics, abstract 972, Vancouver, 1998.

[24] ZEUS Collab., J. Breitweg et al., E. Phys. J.,C2 (1998) 237.

[25] H1 Collab., C. Adloff et al., Z. Phys. C76 (1997) 613.

[26] H. Abramowicz and A. Levy, DESY 97-251, hep-ph/9712415.

[27] J.C. Collins, Phys. Rev. D57 (1998) 3051.

[28] H1 Collab., T. Ahmed et al., Eur. Phys. J. C6 (1999) 421;
ZEUS Collab., J. Breitweg et al., Eur. Phys. J. C5 (1998) 41.

[29] H1 Collab., paper submitted to the 30th International Conference on High-Energy Physics, abstract 960, ICHEP2000, Osaka, Japan, 2000.